

# UC San Diego

## UC San Diego Previously Published Works

### Title

PI3Kgamma activates integrin alpha4 and promotes immune suppressive myeloid cell polarization during tumor progression

### Permalink

<https://escholarship.org/uc/item/7b5375p9>

### Journal

Cancer Immunology Research, 5(11)

### ISSN

2326-6066

### Authors

Foubert, Philippe  
Kaneda, Megan M  
Varner, Judith A

### Publication Date

2017-11-01

### DOI

10.1158/2326-6066.cir-17-0143

Peer reviewed



Published in final edited form as:

*Cancer Immunol Res.* 2017 November ; 5(11): 957–968. doi:10.1158/2326-6066.CIR-17-0143.

## PI3K $\gamma$ activates integrin $\alpha$ 4 promotes immune suppressive myeloid cell polarization during tumor progression

Philippe Foubert<sup>1</sup>, Megan M. Kaneda<sup>1</sup>, and Judith A. Varner<sup>1,2</sup>

<sup>1</sup>Moore's UCSD Cancer Center, University of California, San Diego

<sup>2</sup>Department of Pathology, University of California, San Diego

### Abstract

Immunosuppressive myeloid-derived suppressor cells (MDSCs) and tumor-associated macrophages (TAMs) accumulate in tumors where they inhibit T cell-mediated anti-tumor immune responses and promote tumor progression. Myeloid cell PI3K $\gamma$  plays a key role in regulating tumor immune suppression by promoting integrin  $\alpha$ 4-dependent MDSC recruitment to tumors and by stimulating immune suppressive polarization of MDSCs and TAMs. Here we show that integrin  $\alpha$ 4 promotes immune suppressive polarization of MDSCs and TAMs downstream of PI3K $\gamma$ , thereby inhibiting anti-tumor immunity. Genetic or pharmacological suppression of either PI3K $\gamma$  or integrin  $\alpha$ 4 blocked MDSC recruitment to tumors and also inhibited immune suppressive myeloid cell polarization, thereby significantly reducing expression of IL-10 and increasing expression of IL-12 and IFN $\gamma$  within tumors. Inhibition of PI3K $\gamma$  or integrin  $\alpha$ 4 within tumors stimulated dendritic cell and CD8<sup>+</sup> T cell recruitment and maturation, as well as tumor cell cytotoxicity in vivo, thereby inhibiting tumor growth. As blockade of PI3K $\gamma$  or integrin  $\alpha$ 4 prevents accumulation of MDSC and reduces myeloid cell expression of immunosuppressive factors that stimulate tumor immune escape, these results indicate that PI3K $\gamma$  and integrin  $\alpha$ 4 are valuable targets for the design of novel cancer therapeutics.

### Keywords

Integrin  $\alpha$ 4 $\beta$ 1; PI3K $\gamma$ ; myeloid derived suppressor cell; macrophage; cancer immune suppression

### INTRODUCTION

Chronic inflammation promotes tumor progression by stimulating angiogenesis and suppressing the anti-tumor immune response (1–3). CD11b+Gr1<sup>+</sup> immunosuppressive myeloid cells [myeloid-derived suppressor cells (MDSC)] accumulate in the blood, spleen, lymph nodes, bone marrow and tumor microenvironments in tumor-bearing animals and cancer patients (4–8). These cells, as well as CD11b+Gr1<sup>-</sup> tissue resident macrophages, inhibit innate and adaptive immunity, thereby promoting tumor immune escape (1–8). These immunosuppressive cells inhibit maturation of antigen-presenting dendritic cells (DC),

Correspondence should be addressed to Dr. Judith A. Varner, Moore's UCSD Cancer Center, 3855 Health Sciences Drive, MC0819, La Jolla, CA92093-0819, Phone: (858)-822-0086; Fax: (858)-822-1325, jvarner@ucsd.edu.

The authors declare no competing financial interests.

suppress T cell activation and NK cell cytotoxicity and induce regulatory T cell ( $T_{reg}$ ) development, leading to dysfunctional cell-mediated anti-tumor immunity through the release of immunosuppressive factors such as IL-10, TGF- $\beta$ 1, IL-6, VEGF, and ROS (9–10).

Experimental evidence suggests that therapeutic strategies targeting MDSCs may be beneficial in cancer therapy (11–15). Early studies showed the recruitment, differentiation and expansion of myeloid cells may be modulated in order to promote antitumor immunity and block tumor progression. Strategies targeting the mCSF1 receptor (CSF1R), the CCL2 receptor (CCR2), or PI3K $\gamma$  have been effective in reducing tumor growth and inflammation in animal models and are currently undergoing testing in the cancer patients (11–14). We previously found that CD11b+Gr1+ monocyte and granulocyte trafficking to tumors from circulation depends on PI3K $\gamma$ -mediated activation of integrin  $\alpha$ 4 $\beta$ 1, a receptor for endothelial cell VCAM (14–18). As the most prevalent PI3K isoform in normal myeloid cells, PI3K $\gamma$  is also required for neutrophil motility and trafficking during inflammatory disease (19–20). We found that numerous stimuli activate PI3K $\gamma$  including SDF-1, VEGF-A, IL-4, IL-6, CSF1 and other cytokines and chemokines (17). Once activated, PI3K $\gamma$  stimulates BTK, PLC $\gamma$ , RAPGEF, Rap1a, RIAM and paxillin-dependent integrin  $\alpha$ 4 activation (14–18). Inhibition of PI3K $\gamma$ , BTK, PLC $\gamma$ , RAPGEF, Rap1a, RIAM, or integrin  $\alpha$ 4 $\beta$ 1 suppresses monocyte and granulocyte accumulation in tumors and inhibits tumor growth (14–18).

Recently, we found that PI3K $\gamma$  not only controls myeloid cell trafficking during tumor growth and inflammation, but also controls myeloid cell polarization by regulating immune suppressive gene expression in tumor associated macrophages, monocytes and granulocytes (21–22). Our studies showed that PI3K $\gamma$  stimulates mTor, S6K $\alpha$  and C/EBP $\beta$ -mediated anti-inflammatory gene expression and inhibits NF $\kappa$ B-mediated pro-inflammatory gene expression, thereby promoting expression of immune suppressive factors, such as IL10, TGF $\beta$ , and Arginase and inhibiting expression of IL12, IFN $\gamma$  and Nos2 (21–22). PI3K $\gamma$  activity thereby suppresses T cell immunity and stimulates tumor growth (21). Since our prior studies showed that PI3K $\gamma$  signaling activates integrin  $\alpha$ 4 $\beta$ 1 to promote myeloid cell adhesion and invasion, we speculated that integrin  $\alpha$ 4 $\beta$ 1 might also regulate myeloid cell polarization downstream of PI3K $\gamma$  and thereby affect the anti-tumor immune response.

We show here that integrin  $\alpha$ 4 $\beta$ 1 promotes immune suppressive myeloid cell polarization, inhibits anti-tumor immunity and stimulates tumor growth. Genetic or pharmacologic blockade of integrin  $\alpha$ 4 $\beta$ 1 or its activator PI3K $\gamma$  inhibits immunosuppressive myeloid cell polarization, stimulates dendritic cell maturation and restores anti-tumor T cell mediated immunity in mouse models of cancer. These studies indicate that blockade of the PI3K $\gamma$ -integrin  $\alpha$ 4 pathway is a valuable strategy to suppress tumor growth.

## MATERIALS AND METHODS

### Tumor cell lines

Lewis Lung Carcinoma cells (LLC) were obtained from the American Type Culture collection (ATCC) and cultured in Dulbecco's Modified Medium (DMEM) supplemented with 10% Fetal Bovine Serum (FBS), 2mM glutamine, 100U/ml Penicillin and 100 $\mu$ g/ml

Streptomycin. Pancreatic adenocarcinoma cells (Panc02) were obtained from the David Cheresch laboratory, University of California, San Diego and were cultured in RPMI (GIBCO) supplemented with L-glutamine, 100U/ml Penicillin and 100µg/ml Streptomycin and 10% fetal bovine serum. Cultures were maintained in a humidified incubator at 37°C in an atmosphere containing 5% CO<sub>2</sub>. Both cell lines were verified by RT-PCR or RNA sequencing, in vitro morphological and biochemical criteria and in vivo tumor assays in syngeneic mice.

### Murine macrophage differentiation and culture

Bone marrow derived cells (BMDC) were aseptically harvested from 6–8 week-old female mice by flushing leg bones of euthanized mice with phosphate buffered saline (PBS), 0.5% BSA, 2mM EDTA, incubating in red cell lysis buffer (155 mM NH<sub>4</sub>Cl, 1 mM NaHCO<sub>3</sub> and 0.1 mM EDTA) and centrifuging over Histopaque 1083. Purified mononuclear cells were cultured in RPMI + 20% serum + 50ng/ml M-CSF (PeproTech). Bone marrow derived macrophages were polarized with either IFN $\gamma$  (20 ng/ml, Peprotech) plus LPS (100 ng/ml, Sigma) or LPS alone for 24h or IL-4 (20 ng/ml, Peprotech) for 24–48h. Total RNA was harvested from macrophages using the RNeasy Mini Kit (Qiagen) according to the manufacturer's instructions.

### In vivo tumor studies

Animal studies were approved by the Institutional Animal Care and Use Committee (IACUC), University of California, San Diego.: 5×10<sup>5</sup> LLC cells were injected subcutaneously into syngeneic (C57Bl/6J) 6- to 8- week old wild type (WT), integrin  $\alpha$ 4Y991A, or PI3K $\gamma$ <sup>-/-</sup> (p110 $\gamma$ <sup>-/-</sup>) mice (n=8–10). Tumors dimensions were recorded and excised at 14–21 days. Tumors were cryopreserved in O.C.T., solubilized for RNA purification or collagenase-digested for flow cytometric analysis of immune cell infiltration as detailed below. Alternatively, orthotopic Panc02 pancreatic tumor were initiated by implanting 1×10<sup>6</sup> Panc02 pancreatic carcinoma cells into the pancreas of syngeneic mice (n=8–10). The abdominal cavities of immunocompetent C57Bl/6J mice, integrin  $\alpha$ 4Y991A mutant and PI3K $\gamma$ <sup>-/-</sup> mice were opened and the tails of the pancreas were exteriorized. One million Panc02 cells were injected into the pancreatic tail, the pancreas was placed back into the abdominal cavity, and the incision was closed. Pancreas were excised and cryopreserved after 5 weeks. Tumor weight and immune cell infiltration were quantified as described.

### Drug treatment of tumors

Anti- $\alpha$ 4 mAb blocking antibody studies: C57Bl/6J mice were subcutaneously implanted on day 1 with 0.5×10<sup>6</sup> LLC cells. Mice were treated every third day with intraperitoneally (i.p.) injections of anti- $\alpha$ 4 mAb PS/2 blocking antibody or isotype-matched control rat IgG2b at a dose of 200µg/mouse (10mg/kg) in a 100µl volume (n=8 per group). Tumors were harvested at 14–21 days, weighed and further analyzed by quantitative RT-PCR, flow cytometry and immunohistochemistry. Anti-IL-10 blocking antibody studies: C57Bl/6J mice were subcutaneously implanted on day 1 with 0.5×10<sup>6</sup> LLC cells. Mice were treated on day 7 and day 11 with i.p injections of function-blocking anti-IL10 antibody (JES052A5, R&D Systems) or isotype-matched control antibodies rat IgG1 at a dose of 200µg/mouse (n=6 per group). Tumors were harvested at 14 days, weighed and further analyzed by quantitative RT-

PCR, flow cytometry and immunohistochemistry. PI3K $\gamma$  inhibitor studies: C57Bl/6J mice were subcutaneously implanted on day 1 with  $0.5 \times 10^6$  LLC. Mice were treated by i.p injection with 2.5mg/kg of PI3K $\gamma$  inhibitor (TG100-115) or with a chemically similar inert control (n=10) twice daily for fourteen days for a total daily dose of 5mg/kg. Tumor volumes and weights, as well as myeloid cell densities were measured.

### Isolation of bone marrow derived cells for bone marrow transplantation

Bone marrow cells were aseptically harvested from 6–8 week-old female mice by flushing leg bones of euthanized mice with phosphate buffered saline (PBS) containing 0.5% BSA and 2mM EDTA, incubating cells in red cell lysis buffer and centrifuging over Histopaque 1083. Approximately  $5 \times 10^7$  bone marrow cells were purified by gradient centrifugation from the femurs and tibias of a single mouse. Two million cells were intravenously injected into tail veins of each lethally irradiated (1000rad) 6 week-old syngeneic recipient mouse. After 4 weeks of recovery, tumor cells were injected in BM transplanted animals. LLC (n=8, 3 experiments) tumor growth in C57BL/6 and  $\alpha 4Y991A$  mice transplanted with BM from  $\alpha 4Y991A$  or WT were compared as described above.

### Isolation of tumor-infiltrating immune cells

Tumors were isolated, minced and digested to single cell suspension for 1h at 37°C in 5ml of Hanks Balanced Salt Solution (HBSS, Invitrogen) containing 1mg/ml collagenase type IV (Sigma), 0.1mg/ml hyaluronidase (Sigma) and 20U/ml DNase type IV (Sigma). Cell suspensions were filtered through a 70 $\mu$ m cell strainer and then incubated with different antibodies to perform flow cytometry.

### Flow cytometry

Tumor-infiltrating immune cells were incubated with Fc-blocking reagent (anti CD16/CD32, BD Biosciences), followed by CD11b-APC (M1/70, BD Biosciences), Gr1-FITC (RB6–8C5, BD Biosciences), CD11c-APC (HL3, BD Biosciences), MHC II-FITC (I-Ab, AF6–120.1, BD Biosciences), CD3 -APC (145–2C11, eBioscience), CD4-FITC (GK1.5, eBioscience), CD8a-APC (53–6.7, eBioscience) along with isotype-matched control. In vitro cultures dendritic cells (DCs) were stained with CD11b-APC, Gr1-FITC, CD11c-APC, MHC II-FITC, CD80-FITC (16–10A1, eBioscience) and CD86-FITC (GL1, eBioscience).

### Analysis of gene expression

Total tumor RNA was prepared with TRIzol<sup>®</sup> Reagent (Invitrogen) according to the manufacturer's instructions. In some experiments, total isolated CD11b<sup>+</sup> or CD90.2<sup>+</sup> cells RNA was isolated using RNeasy Mini Kit (Qiagen). cDNA synthesis was performed from 0.5–1 $\mu$ g RNA with SuperScript III First-Strand Synthesis Kit (Invitrogen). Quantitative PCR was performed using primers for *Gapdh*, *Arg1*, *Il10*, *Il6*, *Vegfa*, *Tgfb*, *Il12*, or *Ifng* (QuantiTect Primer Assay). qPCR analysis was performed using a Smart Cycler System (Cepheid).

## Immunohistochemistry

Tumor samples were collected and progressively frozen in cold 2-methylbutane solution. Sections (6µm) were fixed in 100% cold acetone, blocked with 8% normal goat serum for 2 hours, and incubated with the appropriate primary antibodies (rat anti-mouse CD11b, Hamster anti-mouse CD11c, rat anti-mouse CD8a or rat anti-mouse CD11b, BD Biosciences) for 2 hours at room temperature. Sections were washed 3 times with PBS and incubated with goat anti-rat secondary antibodies coupled to Alexa488 or 597 for CD11b, CD8 and CD4 studies or with Cy5-goat anti-Hamster for CD11c studies. Nuclei were stained with 4',6-diamidino-2-phenylindole (DAPI). The slides were washed and mounted in DAKO fluorescent mounting medium. The detection of apoptotic cells was performed using a TUNEL-assay (ApoTag Fluorescein In Situ Apoptosis Detection Kit, Promega) in accordance with the manufacturer's instructions. Immunofluorescence images were collected on a Nikon microscope (Eclipse TE2000-U) and pixels of fluorescence or area of staining was quantified using MetaMorph Software.

## Isolation of tumor-infiltrating myeloid cells and T cells

Myeloid CD11b<sup>+</sup> cells and CD90.2<sup>+</sup> (Thy1.2) T cells were isolated from tumor cell suspensions using CD11b or CD90.2 microbeads (Miltenyi Biotech), respectively. The purity of the sorted cells was typically >80% as assessed by FACS analysis. In some experiments, tumor-infiltrating lymphocytes were stained with CD4-FITC (GK1.5, eBioscience) and CD8-APC (53-6.7, eBioscience).

## In vitro cytotoxicity assay

Thy1.2<sup>+</sup> T cells (effector cells) in tumor were purified from LLC tumor-bearing WT and α4Y991A mice and then co-incubated with LLC tumor cells (target cells) at 2.5:1, 5:1 and 10:1 ratios (2×10<sup>3</sup> LLC tumor cells per well) for 6 hours. Target cell killing was assayed by collecting the supernatants from each well for measurement of the lactate dehydrogenase release (Cytotox96 NonRadioactive Cytotoxicity Assay kit, Promega).

## Effect of T cells from mice bearing tumors on tumor cell killing *in vivo*

CD90.2<sup>+</sup> T cells were first isolated from the spleens of WT, α4Y991A and PI3Kγ<sup>-/-</sup> mice bearing tumors using the MACS system and then mixed with viable LLC tumor cells at ratio 1:2. The mixture was injected into the flanks of naïve mice. Tumor growth, intratumoral apoptosis and necrosis were investigated after 10 days.

## IL-10 Elisa

Tumors were collected and homogenized in RIPA lysis buffer (137mM NaCl, 20mM Tris-HCL pH8, 10% Glycerol, 1% Triton X-100, 0.1% SDS and protease inhibitor cocktail). Protein extracts were clarified by centrifugation at 12,000 *g* for 10 minutes at 4°C, and clarified protein samples were used for IL-10 ELISA quantification (R&D Systems).

## Statistical Analysis

Results were expressed as mean  $\pm$  SEM. Data comparing differences between two groups were assessed using unpaired Student's t-test. One-way ANOVA with post hoc testing was used for multiple comparisons. A value of  $P < 0.05$  was considered significant.

## RESULTS

### Inhibition of PI3K $\gamma$ or integrin $\alpha 4$ inhibits CD11b+Gr1+ MDSC accumulation and tumor progression

Tumor inflammation promotes the accumulation of CD11b+Gr1+ MDSCs and CD11b+Gr1-TAMs that inhibit anti-tumor immunity, thereby favoring tumor progression (4–8). We previously found that recruitment of circulating Gr1+ myeloid cells into tumors is regulated by PI3K $\gamma$ -mediated integrin  $\alpha 4\beta 1$  activation (14–18). We also found that PI3K $\gamma$  directly promotes TAM polarization by activating an mTor, S6K $\alpha$  and C/EBP $\beta$ -dependent transcriptional pathway, leading to expression of immune suppressive factors, such as Arginase, IL10 and TGF $\beta$  that directly promote tumor immune suppression (21–22). As integrin  $\alpha 4\beta 1$  is downstream of PI3K $\gamma$ , we speculated that integrin  $\alpha 4\beta 1$  might also regulate immune suppressive transcription in myeloid cells.

To investigate whether integrin  $\alpha 4$  regulates immune suppressive myeloid cell polarization in tumors, we first compared tumor growth and inflammation in two different models of tumor growth, the syngeneic subcutaneous Lewis Lung Carcinoma (LLC) and orthotopic Panc02 pancreatic adenocarcinoma (PDAC) models in WT, PI3K $\gamma^{-/-}$  or  $\alpha 4Y991A$  knockin mice and in mice treated with inhibitors of integrin  $\alpha 4$  or PI3K $\gamma^{-/-}$  (Fig. 1). Integrin  $\alpha 4Y991A$  mice express a knockin point mutation in the  $\alpha 4$  cytoplasmic tail that inhibits integrin activation, which we previously showed is controlled by PI3K $\gamma$  signaling in myeloid cells (17). LLC and Panc02 tumors implanted in integrin  $\alpha 4Y991A$  and PI3K $\gamma^{-/-}$  mice were both significantly smaller than tumors implanted in control treated mice ( $P < 0.001$ ), whether analyzed at endpoint or over time (Fig. 1A-C). Growth of lung LLC tumors was similarly inhibited in animals treated with inhibitors of  $\alpha 4$  or PI3K $\gamma$ : PS2, an anti- $\alpha 4$  function-blocking antibody (anti- $\alpha 4$ ) or TG100–115, a PI3K $\gamma$  inhibitor (Fig. 1A, Supplementary Figure 1). Flow cytometric analyses of LLC or Panc02 tumors implanted in WT, integrin  $\alpha 4Y991A$  and PI3K $\gamma^{-/-}$  mice revealed significant reductions in infiltration of total CD11b+Gr1+ myeloid cells (Fig. 1D-F), as well as in CD11b+Gr1lo and CD11b+Gr1hi myeloid cell subpopulations but not of CD11bGr1-cells (Fig. 1G) in PI3K $\gamma^{-/-}$  and  $\alpha 4Y991A$  animals compared with WT animals. These populations were further defined by marker analysis as CD11b+Gr1loLy6G-F4/80loCD206-CD11c- monocytes, CD11b+Gr1hiLy6G+F4/80-CD206-CD11c- granulocytes and CD11b+Gr1-Ly6G-F4/80hiCD206+CD11c+ (Fig. 1H). Similar results were observed in tumor-bearing mice treated with the anti- $\alpha 4$  blocking antibody or with the PI3K $\gamma$  inhibitor TG100–115 (Fig. 1D-G). These data show that loss of PI3K $\gamma$  or integrin  $\alpha 4$  activity affects trafficking of Gr1+ but not Gr1-myeloid cells.

Surprisingly, tumors from PI3K $\gamma^{-/-}$  and  $\alpha 4Y991A$  animals not only exhibited decreased CD11b+ cell infiltration but also increased CD11c+ dendritic cell infiltration in tumors and



lymph nodes compared to control animals (Figure 2A-C). Similar results were observed in  $\alpha 4Y991A$  mice transplanted with mice transplanted with  $\alpha 4Y991A$  bone marrow but not in mice transplanted with WT bone marrow (Fig. 2D-F). Importantly, the percentages of mature MHCII-expressing dendritic cells (CD11c<sup>+</sup>MHCII<sup>+</sup>) increased in  $\alpha 4Y991A$  and PI3K $\gamma^{-/-}$  Panc02 and LLC tumors compared to WT tumors ( $P < 0.01$ ) and in tumors from animals that were treated with anti- $\alpha 4$  blocking antibody or the PI3K $\gamma$  inhibitor TG100-115 (Fig. 2G-I). The ratio of MHCII<sup>+</sup> mature DC to MHCII<sup>-</sup>immature DC was 2-fold higher in tumors from these mice compared to control mice ( $P < 0.001$ ) (Fig. 2J-K). In addition, levels of the co-stimulatory protein CD80 were significantly higher in dendritic cells in tumors from PI3K $\gamma^{-/-}$  and  $\alpha 4Y991A$  animals (Fig. 2L). Together, these results indicate that PI3K $\gamma$  and  $\alpha 4$  integrin inhibit dendritic cell recruitment and maturation in association with tumor inflammation and growth and that inhibitory targeting of these molecules can stimulate dendritic cell recruitment and activation.

### Integrin $\alpha 4$ regulates myeloid cell polarization

We previously found that PI3K $\gamma$  promotes immune suppressive transcription in TAMs and MDSCs, thereby contributing to tumor immune escape (18, 21-22). Therefore, as integrin  $\alpha 4$  is directly downstream of PI3K $\gamma$ , we investigated the role of integrin  $\alpha 4$  in myeloid cell polarization. We used RT-PCR to assess the expression of pro- and anti-inflammatory factors in LLC and Panc02 tumors from WT,  $\alpha 4Y991A$  and PI3K $\gamma^{-/-}$  mutant mice and in LLC tumors from anti- $\alpha 4$  and TG100-115 treated mice. We observed increased expression of immunostimulatory cytokines, such as *Il12b* and *Ifng* and decreased mRNA expression of immune suppressive and pro-angiogenic factors, such as *Il10*, *Il6*, *Arg1*, and *VEGFa* in LLC and Panc02 tumors from  $\alpha 4Y991A$  and PI3K $\gamma^{-/-}$  mice (Fig. 3A-B). Treatment of LLC tumors with an anti- $\alpha 4$  blocking antibody or a PI3K $\gamma$  inhibitor (TG100-115) had similar effects on inflammatory factor expression (Fig. 3C-D). These gene expression changes were also observed in tumor associated CD11b<sup>+</sup> myeloid cells purified from  $\alpha 4Y991A$  and PI3K $\gamma^{-/-}$  mice (Fig. 3E).

To determine whether integrin  $\alpha 4\beta 1$ , like PI3K $\gamma$ , plays a fundamental role in controlling macrophage polarization, we also performed gene expression analyses on *in vitro* cultured, IL-4 stimulated macrophages derived from bone marrow of WT and  $\alpha 4Y991A$  mice. We found that loss of integrin activity in  $\alpha 4Y991A$  macrophages suppressed expression of *Il10*, *Arg1* and *Tgfb1* and stimulated expression of immune stimulatory factor mRNA, such as *Il12* and *Ifng* *in vitro* (Fig. 3F). As IL-4 stimulated macrophages closely resemble tumor-derived macrophages (21), our results indicate that integrin  $\alpha 4\beta 1$  plays a role in the PI3K $\gamma$  signaling cascade that regulates myeloid cell polarization. Taken together, these results suggest that integrin  $\alpha 4$  regulates immunosuppressive myeloid cell transcription downstream of PI3K $\gamma$  during tumor inflammation.

IL10 is a key immune suppressive factor expressed by TAMs, MDSCs and other immune cells; it impairs DC maturation and effector T cell function (10). We observed that CD11b<sup>+</sup> myeloid cells are the principal source of *Il10* expression in LLC tumors (Fig. 4A). Importantly, IL10 protein and RNA expression was suppressed in  $\alpha 4Y991A$  MDSCs and in tumors from  $\alpha 4Y991A$  BM transplanted animals (Fig. 4B-C). As integrin  $\alpha 4$  activity



promotes IL10 expression, we further elucidated the role of IL-10 in the control of DC maturation during tumor growth. Mice bearing LLC tumors were treated over the course of 10 days with anti-IL10 blocking antibodies. Although this treatment did not significantly affect tumor growth, it did increase the total percentage of intratumoral mature MHCII+ DC compared to treatment with control isotype-matched antibody (Fig. 4D-F). Importantly, mice treated with anti-IL10 blocking antibodies exhibited increased expression of *Iil2b*, *Ifng* and *Cd8a* mRNA (Fig. 4G-I) as well as increased infiltration of CD8+ T cells as detected by IHC (Fig. 4J-K). Together, these data suggest that the integrin  $\alpha 4$  regulated production of IL-10 by CD11b+ myeloid cells prevents DC maturation and inhibits anti-tumor T cell responses.

### PI3K $\gamma$ -integrin $\alpha 4$ pathway inhibits CD8+ T cell recruitment and activation in the tumor microenvironment

To promote an effective anti-tumor immune response, tumor-specific T cells must be present in sufficient numbers to kill their targets. A direct correlation exists between the number of tumor-infiltrating lymphocytes (TILs) and a favorable clinical outcome (23–26). Furthermore, the functional status of TILs has been correlated with a favorable prognosis in human malignancies (25–26). To further understand the mechanisms underlying the immune suppression mediated by inhibition of PI3K $\gamma$ -integrin  $\alpha 4$  pathway, we evaluated whether blockade of this pathway alters both the number and the activation state of the tumor-infiltrating lymphocytes. Histological examination of tumors revealed reduced CD4+ T cells and increased CD8+ T cells in tumors from both  $\alpha 4Y991A$  and PI3K $\gamma^{-/-}$  mice when compared to WT mice (Fig. 5A-B). Additionally, flow cytometric analysis of tumor-infiltrating lymphocytes isolated from tumors showed that CD4+ T cells were reduced, while CD8+ T cells were increased, in  $\alpha 4Y991A$  and PI3K $\gamma^{-/-}$  mice compared to WT mice (Fig. 5C-D). These observations were supported by increases in total *Cd8a* mRNA in tumors from both  $\alpha 4Y991A$  and PI3K $\gamma^{-/-}$  mice when compared to WT mice (Fig. 5E). Importantly, TILs from  $\alpha 4Y991A$  and PI3K $\gamma^{-/-}$  mice expressed more *Ifng* and less *Tgfb1* and *Iil10* than WT TILs, suggesting that inhibition of myeloid cell PI3K $\gamma$  or integrin  $\alpha 4\beta 1$  resulted in increased recruitment and priming of CD8+ T cells in tumors (Fig. 5F). To determine whether myeloid cell PI3K $\gamma$  or integrin  $\alpha 4\beta 1$  promote T cell mediated tumor cell killing, TILs isolated from WT,  $\alpha 4Y991A$  or PI3K $\gamma^{-/-}$  mice were co-cultured with LLC cells in a direct *ex vivo* CTL assay. TILs from  $\alpha 4Y991A$  or PI3K $\gamma^{-/-}$  mutant mice exhibited a 2–3 fold increase in LLC tumor cell cytotoxicity than TILs from WT mice (Fig. 5G).

To determine whether PI3K $\gamma$  and  $\alpha 4$  integrin also suppress T cell mediated cytotoxicity *in vivo*, we mixed tumor-infiltrating T lymphocytes isolated from tumors of WT,  $\alpha 4Y991A$  or PI3K $\gamma^{-/-}$  mice with LLC tumor cells and injected the mixture into the flanks of C57Bl/6J naïve mice. When LLC tumor cells were mixed with  $\alpha 4Y991A$  and PI3K $\gamma^{-/-}$  T cells, tumor dimensions and weights were markedly reduced compared to tumors derived from LLC cells mixed with WT T cells ( $P < 0.001$ ) (Fig. 6A-B). Tumors derived from LLC cells mixed  $\alpha 4Y991A$  and PI3K $\gamma^{-/-}$  T cells exhibited increased intratumoral cell death, as detected by *in situ* TUNEL assay (Fig. 6C-D) and H&E staining (Figure 6E-F) in mice injected with  $\alpha 4Y991A$  and PI3K $\gamma^{-/-}$  T cells compared to mice receiving WT T cells. Together, these studies show that integrin  $\alpha 4\beta 1$ , like PI3K $\gamma$ , suppresses T cell mediated

tumor cell cytotoxicity and inhibiting the PI3K $\gamma$ -integrin  $\alpha 4\beta 1$  pathway can stimulate T cell cytotoxicity.

These studies indicate that myeloid cell PI3K $\gamma$  and integrin  $\alpha 4^{-/-}$  regulate myeloid cell polarization to control anti-tumor T cell activation. In summary, these data show that blocking the PI3K $\gamma$ - $\alpha 4$  integrin pathway in myeloid cells can restore anti-tumor immunity by modulating the tumor microenvironment and promoting tumor cell killing by T cells. We present here the completely new concept that integrin  $\alpha 4\beta 1$  regulates myeloid cell polarization and anti-tumor immunity and that inhibition of this PI3K $\gamma$ -integrin  $\alpha 4$  pathway could be a useful therapeutic approach to stimulate anti-tumor immunity.

## Discussion

We previously demonstrated the specific roles of integrin  $\alpha 4$  and PI3K $\gamma$  in the trafficking of myeloid cells to sites of tumor inflammation (14–18; 21–22). Here, we extend these observations to demonstrate a new role for integrin  $\alpha 4\beta 1$  in the control of myeloid cell polarization during tumor progression. Our studies demonstrate that integrin  $\alpha 4$ , like PI3K $\gamma$ , not only regulates myeloid cell trafficking to tumors but also promotes immune suppressive myeloid cell polarization, inhibition of anti-tumor immunity and stimulation of tumor growth. We previously showed that PI3K $\gamma$  stimulates BTK-, PLC $\gamma$ -, RAPGEF-, Rap1a-, RIAM- and paxillin-dependent integrin  $\alpha 4$  activation (14–18). We also previously showed that PI3K $\gamma$  activates BTK to promote immune suppressive myeloid cell polarization, by inducing mTor, S6K $\alpha$ , or C/EBP $\beta$  dependent expression of IL10, TGF $\beta$ , and Arginase, and inhibiting expression of IL12, IFN $\gamma$  and Nos2 (18, 21–22). Interestingly, cEBPbeta has been previously shown to control immune suppression in tumor-infiltrating myeloid cells and (27). Our present studies show that a PI3K $\gamma$ -integrin  $\alpha 4$  pathway inhibits anti-tumor immunity through stimulation of CD11b+Gr1+ cell recruitment and immunosuppressive myeloid cell polarization. Although it is not currently clear whether integrin  $\alpha 4$  directly participates in PI3K $\gamma$ -mediated activation of mTor, S6K $\alpha$ , or C/EBP $\beta$ , these findings establish a new role for a PI3K $\gamma$ -integrin  $\alpha 4$  pathway as a critical modulator of tumor inflammation and immunosuppression.

Several lines of evidence presented here support that blockade of this pathway is critical to regulate anti-tumor immune responses. First, inhibition of the PI3K $\gamma$ -integrin  $\alpha 4$  pathway is associated with reduction of CD11b+Gr1+ MDSC infiltration and immunosuppressive factors (IL10, IL6, TGF $\beta$ , or Arginase) in the tumor microenvironment and lymph nodes of tumor-bearing animals. Importantly, our data also showed that blocking this pathway reduces immunosuppressive factors expressed in tumor-infiltrating CD11b+ myeloid cells.

Second, disruption of the PI3K integrin  $\gamma$ - $\alpha 4$  pathway increased the recruitment of mature DCs into the tumor microenvironment and into the draining LN. Defects in dendritic cells caused by the immunosuppressive tumor microenvironment result in the accumulation of immature DC. These immature DC can directly promote tumor angiogenesis (28–36) and suppress T cell responses (10), thus favoring tumor progression. We observed that blockade of a PI3K $\gamma$ - $\alpha 4$  integrin pathway could facilitate CD11c dendritic cell infiltration and maturation. DC differentiation and maturation depends on factors produced by the

microenvironment, such as IL-10. Our results showed that PI3K $\gamma$  and integrin  $\alpha$ 4 regulate IL-10 production by CD11b<sup>+</sup> cells and thereby regulate DC differentiation and maturation.

Third, blockade of the PI3K $\gamma$ - integrin  $\alpha$ 4 pathway increased expression of immunostimulatory cytokines (IL12 $\beta$ , IFN $\gamma$ ), reduced CD4<sup>+</sup> T cell infiltration and promoted CD8<sup>+</sup> T cell accumulation into the tumor microenvironment. Furthermore, inhibition of this pathway promoted T cell-mediated tumor cytotoxicity and tumor rejection. As shown in Figure 5, we do not observe fewer T cells, but rather more T cells, in tumors from  $\alpha$ 4Y991A and PI3K $\gamma^{-/-}$  mice. Our studies show that integrin  $\alpha$ 4 does not control T cell trafficking to tumors. Importantly, we and others demonstrated that PI3K $\gamma$  deficiency increases CD8<sup>+</sup> cell differentiation and Th1 cytokine production (IL12, IFN $\gamma$ ) but does not directly affect Th1/Th2 T cell polarization (22).

Finally, the PI3K $\gamma$ - $\alpha$ 4 integrin pathway also affects tumor progression by promoting angiogenesis (17). Myeloid cells can support tumor angiogenesis and growth through the production of proangiogenic factors (28–32). Interestingly, we found that blockade of the PI3K $\gamma$ -integrin  $\alpha$ 4 pathway reduced expression of proangiogenic factors and tumor angiogenesis. Inhibition of this pathway increased myeloid cell expression of IL12, a principal Th1 cytokine that harbors potent anti-angiogenic activity (33–34). Therefore, inhibition of PI3K $\gamma$  and integrin  $\alpha$ 4 can control tumor angiogenesis and immunity.

In addition, inhibition of the PI3K $\gamma$ - $\alpha$ 4 integrin pathway could influence the development of regulatory T cells (Treg), a key player in the maintenance of tumor immune tolerance (34). In fact, we found that TGF $\beta$ , a cytokine that induces the generation of Treg (35) was down-regulated in T cells from PI3K $\gamma$  and  $\alpha$ 4 integrin mutant mice, suggesting that disruption of this pathway reduces the generation of Treg in the tumor microenvironment.

The tumor microenvironment represents a consistently effective barrier to immune cell function. Our results indicate that blocking the PI3K $\gamma$ -integrin  $\alpha$ 4 pathway can inhibit the immunosuppressive tumor microenvironment and promote anti-tumor immunity. The present findings support the development of novel strategies based on the inhibition of PI3K $\gamma$ -integrin  $\alpha$ 4 pathway to control tumor immune suppression.

## Supplementary Material

Refer to Web version on PubMed Central for supplementary material.

## Acknowledgements

We thank the Moores UCSD Cancer Center Flow Cytometry and Histology Shared Resources for technical assistance.

### Grant Support

This research was supported by fellowships from the “Fondation pour la Recherche Medical”, the “Fondation Bettencourt-Schueller” and the Pancreatic Cancer Action Network-AACR to Philippe Foubert and NIH grants R01CA83133 and R01CA167426 Judith A. Varner.

## REFERENCES

1. Sica A, Mantovani A. Macrophage plasticity and polarization: in vivo veritas. *J Clin Invest* 2012;122: 787–95. [PubMed: 22378047]
2. Schmid MC, Varner JA. Myeloid cells in tumor inflammation. *Vasc Cell* 2012;4: 14. [PubMed: 22938502]
3. Wynn TA, Chawla A, Pollard JW. Macrophage biology in development, homeostasis and disease. *Nature* 2013;496:445–455. [PubMed: 23619691]
4. Nagaraj S, Youn JI, Gabrilovich DI. Reciprocal relationship between myeloid-derived suppressor cells and T cells. *J Immunol* 2013;191: 17–23. [PubMed: 23794702]
5. Kumar V, Patel S, Tcyganov E, Gabrilovich DI. The Nature of Myeloid-Derived Suppressor Cells in the Tumor Microenvironment. *Trends Immunol* 2016;37: 208–220. [PubMed: 26858199]
6. Gabrilovich DI. Myeloid-Derived Suppressor Cells. *Cancer Immunol Res* 2017;5:3–8. [PubMed: 28052991]
7. Bronte V, Brandau S, Chen SH, Colombo MP, Frey AB, Greten TF, et al. Recommendations for myeloid-derived suppressor cell nomenclature and characterization standards. *Nat Commun* 2016;7:12150. [PubMed: 27381735]
8. Kumar V, Patel S, Tcyganov E, Gabrilovich DI. The Nature of Myeloid-Derived Suppressor Cells in the Tumor Microenvironment. *Trends Immunol* 2016;37:208–20. [PubMed: 26858199]
9. Ito M, Minamiya Y, Kawai H, Saito S, Saito H, Nakagawa T, et al. Tumor-derived TGFbeta-1 induces dendritic cell apoptosis in the sentinel lymph node. *J Immunol* 2006;176: 5637–43. [PubMed: 16622033]
10. Ruffell B, Chang-Strachan D, Chan V, Rosenbusch A, Ho CM, Pryer N, et al. Macrophage IL-10 blocks CD8+ T cell-dependent responses to chemotherapy by suppressing IL-12 expression in intratumoral dendritic cells. *Cancer Cell* 2014;26:623–37. [PubMed: 25446896]
11. Sandhu SK, Papadopoulos K, Fong PC, Patnaik A, Messiou C, Olmos D, et al. A first-in-human, first-in-class, phase I study of carlumab (CNTO 888), a human monoclonal antibody against CC-chemokine ligand 2 in patients with solid tumors. *Cancer Chemother Pharmacol* 2013;71:1041–50. [PubMed: 23385782]
12. Pyonteck SM, Akkari L, Schuhmacher AJ, Bowman RL, Sevenich L, Quail DF, et al. CSF-1R inhibition alters macrophage polarization and blocks glioma progression. *Nat Med* 2013;19: 1264–72. [PubMed: 24056773]
13. Zhu Y, Knolhoff BL, Meyer MA, Nywening TM, West BL, Luo J, et al. CSF1/CSF1R blockade reprograms tumor-infiltrating macrophages and improves response to T-cell checkpoint immunotherapy in pancreatic cancer models. *Cancer Res* 2014;74: 5057–69. [PubMed: 25082815]
14. Jin H, Su J, Garmy-Susini B, Kleeman J, Varner J. Integrin alpha4beta1 promotes monocyte trafficking and angiogenesis in tumors. *Cancer Res* 2006;66:2146–52. [PubMed: 16489015]
15. Schmid MC, Avraamides CJ, Foubert P, Shaked Y, Kang SW, Kerbel RS, et al. Combined blockade of integrin- $\alpha 4\beta 1$  plus cytokines SDF-1 $\alpha$  or IL-1 $\beta$  potently inhibits tumor inflammation and growth. *Cancer Res* 2011;71:6965–75. [PubMed: 21948958]
16. Schmid MC, Franco I, Kang SW, Hirsch E, Quilliam LA, Varner JA. PI3-kinase  $\gamma$  promotes Rap1a-mediated activation of myeloid cell integrin  $\alpha 4\beta 1$ , leading to tumor inflammation and growth. *PLoS One* 2013;8:e60226. [PubMed: 23565202]
17. Schmid MC, Avraamides CJ, Dippold HC, Franco I, Foubert P, Ellies LG, et al. Receptor tyrosine kinases and TLR/IL1Rs unexpectedly activate myeloid cell PI3k $\gamma$ , a single convergent point promoting tumor inflammation and progression. *Cancer Cell* 2011;19: 715–27. [PubMed: 21665146]
18. Gunderson AJ, Kaneda MM, Tsujikawa T, Nguyen AV, Affara NI, Ruffell B, et al. Bruton Tyrosine Kinase-Dependent Immune Cell Cross-talk Drives Pancreas Cancer. *Cancer Discov* 2015; 6: 270–285. [PubMed: 26715645]
19. Hirsch E, Katanaev VL, Garlanda C, Azzolino O, Pirola L, Silengo L, et al. Central role for G protein-coupled phosphoinositide 3-kinase  $\gamma$  in inflammation. *Science* 2000; 287:1049–53. [PubMed: 10669418]

20. Sasaki T, Irie-Sasaki J, Jones RG, Oliveira-dos-Santos AJ, Stanford WL, Bolon B, et al. Function of PI3K $\gamma$  in thymocyte development, T cell activation, and neutrophil migration. *Science* 2000;287:1040–6. [PubMed: 10669416]
21. Kaneda MM, Messer KS, Ralainirina N, Li H, Leem CJ, Gorjestani S, et al. PI3K $\gamma$  is a molecular switch that controls immune suppression. *Nature* 2016;539:437–442. [PubMed: 27642729]
22. Kaneda MM, Cappello P, Nguyen AV, Ralainirina N, Hardamon CR, Foubert P, et al. Macrophage PI3K $\gamma$  Drives Pancreatic Ductal Adenocarcinoma Progression. *Cancer Discov* 2016;6:870–85. [PubMed: 27179037]
23. Zhang L, Conejo-Garcia JR, Katsaros D, Gimotty PA, Massobrio M, Regnani G, et al. Intratumoral T cells, recurrence, and survival in epithelial ovarian cancer. *N Engl J Med* 2003;348:203–13. [PubMed: 12529460]
24. DeNardo DG, Andreu P, Coussens LM., Interactions between lymphocytes and myeloid cells regulate pro-versus anti-tumor immunity. *Cancer Metastasis Rev* 2010; 29: 309–16. [PubMed: 20405169]
25. Naito Y, Saito K, Shiiba K, Ohuchi A, Saigenji K, Nagura H, et al. CD8+ T cells infiltrated within cancer cell nests as a prognostic factor in human colorectal cancer. *Cancer Res* 1998; 58: 3491–4. [PubMed: 9721846]
26. Schumacher K, Haensch W, Röefzaad C, Schlag PM. Prognostic significance of activated CD8(+) T cell infiltrations within esophageal carcinomas. *Cancer Res* 2001; 61: 3932–6. [PubMed: 11358808]
27. Marigo I, Bet al., Tumor-induced tolerance and immune suppression depend on the C/EBP $\beta$  transcription factor. *Immunity* 2010; 32:790–802. [PubMed: 20605485]
28. Fainaru O, Adini A, Benny O, Adini I, Short S, Bazinet L, et al., Dendritic cells support angiogenesis and promote lesion growth in a murine model of endometriosis. *Faseb J* 2008; 22: 522–9. [PubMed: 17873101]
29. Fainaru O, Almog N, Yung CW, Nakai K, Montoya-Zavala M, Abdollahi A, et al. Tumor growth and angiogenesis are dependent on the presence of immature dendritic cells. *Faseb J* 2010;24:1411–8. [PubMed: 20008545]
30. Murdoch C, Muthana M, Coffelt SB, Lewis CE. The role of myeloid cells in the promotion of tumour angiogenesis. *Nat Rev Cancer* 2008; 8: 618–31. [PubMed: 18633355]
31. Yang L, DeBusk LM, Fukuda K, Fingleton B, Green-Jarvis B, Shyr Y, et al. Expansion of myeloid immune suppressor Gr<sup>+</sup>CD11b<sup>+</sup> cells in tumor-bearing host directly promotes tumor angiogenesis. *Cancer Cell* 2004; 6: 409–21. [PubMed: 15488763]
32. Schmid MC, Varner JA. Myeloid cells in the tumor microenvironment: modulation of tumor angiogenesis and tumor inflammation. *J Oncol* 2010;2010:201026.
33. Trinchieri G, Interleukin-12 and the regulation of innate resistance and adaptive immunity. *Nat Rev Immunol* 2003; 3: 133–46. [PubMed: 12563297]
34. Del Vecchio M, Bajetta E, Canova S, Lotze MT, Wesa A, Parmiani G, et al. Interleukin-12: biological properties and clinical application. *Clin Cancer Res* 2007; 13: 4677–85. [PubMed: 17699845]
35. Zou W Regulatory T cells, tumour immunity and immunotherapy. *Nat Rev Immunol* 2006; 6: 295–307. [PubMed: 16557261]
36. Wrzesinski SH, Wan YY, Flavell RA. Transforming growth factor-beta and the immune response: implications for anticancer therapy. *Clin Cancer Res* 2007; 13: 5262–70. [PubMed: 17875754]

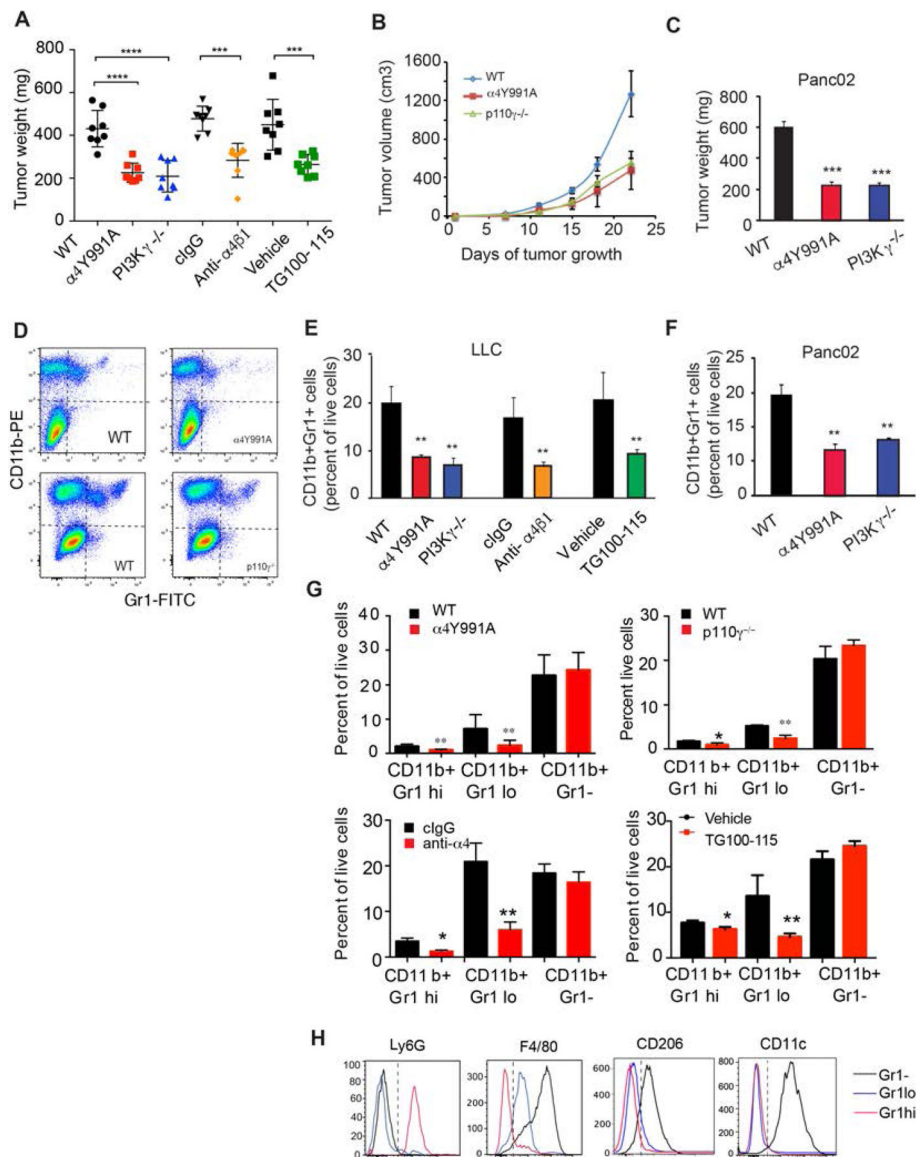


**Figure 1: PI3K $\gamma$  and integrin  $\alpha 4$  similarly impact tumor progression and CD11b+Gr1+ MDSC infiltration.**

(A) Weights of LLC tumors implanted in WT versus  $\alpha 4Y991A$  or PI3K $\gamma^{-/-}$  animals and of tumors that were treated with anti- $\alpha 4$  blocking or isotype antibodies (10mg/kg every 3 days) or with the PI3K $\gamma$  inhibitor TG100-115 or vehicle ( $****p < 0.0001$ ) (n=10). (B) Time course of LLC tumor growth in WT versus  $\alpha 4Y991A$  or PI3K $\gamma^{-/-}$  animals (n=10). (C) Weights of orthotopic Panc02 pancreatic adenocarcinoma tumors from WT,  $\alpha 4Y991A$  or PI3K $\gamma^{-/-}$  animals ( $***p < 0.001$ ) (n=10). (D) Representative FACS profiles of CD11b+ myeloid cell populations in LLC tumors from WT,  $\alpha 4Y991A$ , and PI3K $\gamma^{-/-}$  mice from A ( $**p < 0.01$ ). (E) Quantification of CD11b+Gr1+ myeloid cells as a percent of live cells in tumors from A (n=4). (F) Quantification of CD11b+Gr1+ myeloid cells as a percent of live cells from C ( $**p < 0.01$ ) (n=4). (G) Quantification of CD11b+Gr1hi neutrophils, CD11b+Gr1lo monocytes and CD11b+Gr1- macrophages as a percent of live cells in tumors from A (n=4) ( $*p < 0.05$ ;  $**p < 0.01$ ). (H) FACS profiles of Ly6G, F4/80, CD206 and CD11c in the three



myeloid cell populations observed in D and quantified in G. Similar results were obtained in 3 replicate experiments. Error bars indicate standard error of the mean (SEM).

Author Manuscript

Author Manuscript

Author Manuscript

Author Manuscript



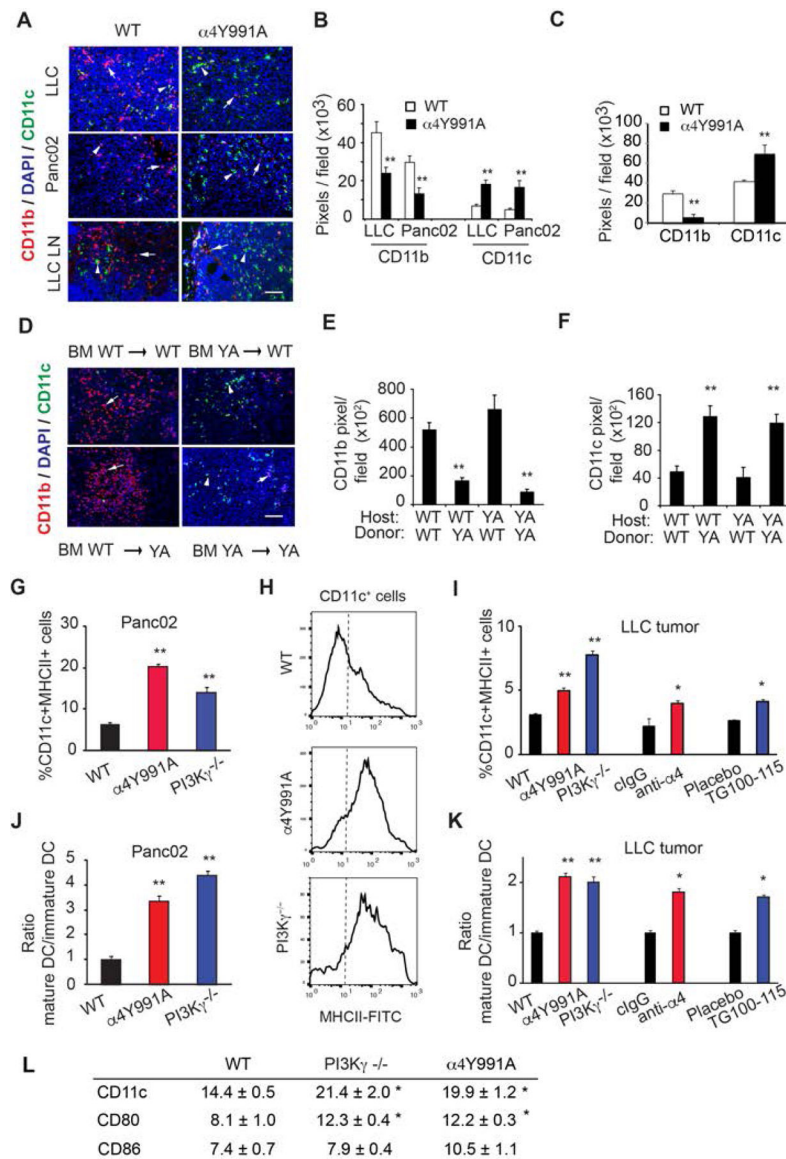


**Figure 2. Blockade of PI3K $\gamma$ -integrin  $\alpha 4$  pathway promotes infiltration and maturation of CD11c<sup>+</sup> dendritic cell in the tumor microenvironment.**

(A) Representative images of CD11c<sup>+</sup> dendritic cells (green, arrowhead) and CD11b<sup>+</sup> myeloid cells (red, arrow) in cryosections from LLC and Panc02 tumors and LLC tumor draining lymph nodes from WT and  $\alpha 4Y991A$  mice. Scale bar: 100 $\mu$ m. (B) Quantitative analysis of CD11b<sup>+</sup> and CD11c<sup>+</sup> cells in LLC and Panc02 tumors in WT and  $\alpha 4Y991A$  mice from A, expressed as pixels per field (n=5). \*\* $p < 0.01$  vs WT. (C) Quantitative analysis of CD11b<sup>+</sup> and CD11c<sup>+</sup> cells in LLC tumor draining lymph nodes in WT and  $\alpha 4Y991A$  mice from A, expressed as pixels per field (n=5). \*\* $p < 0.01$  vs WT. Scale bar: 100 $\mu$ m. (D) Representative images of CD11c<sup>+</sup> dendritic cells and CD11b<sup>+</sup> myeloid cells in LLC tumors implanted in integrin  $\alpha 4Y991A$  mice transplanted with WT or  $\alpha 4Y991A$  BM and in WT mice transplanted with  $\alpha 4Y991A$  or WT BM. Scale bar: 100 $\mu$ m. (E-F) Quantitative analysis of (E) CD11b<sup>+</sup> and (F) CD11c<sup>+</sup> pixels in tumors from D (n=5). (G) Quantitative analysis of CD11c<sup>+</sup>MHCII<sup>+</sup> mature dendritic cells in Panc02 tumors assessed by flow cytometry in

WT,  $\alpha 4Y991A$ , and  $PI3K\gamma^{-/-}$  mice (n=5).  $**p<0.01$  vs WT. **(H)** Representative FACs plots of MHCII expression in  $CD11c^+$  cells from **G**. **(I)** Quantification of  $CD11c^+MHCII^+$  mature DC infiltration in LLC tumors assessed by flow cytometry in WT,  $\alpha 4Y991A$ , and  $PI3K\gamma^{-/-}$  mice and mice treated with anti- $\alpha 4$  antibody or  $PI3K\gamma$  inhibitor TG100-115 (n=5),  $**p<0.01$ . **(J-K)** Quantification of the ratio between mature DC ( $CD11c^+/MHCII^+$ ) and immature DC ( $CD11c^+/MHCII^-$ ) in Panc02 **(J)** and LLC **(K)** tumors from **(G and I)** (n=5)  $*p<0.05$ ,  $**p<0.01$ . Error bars indicate standard error of the mean (SEM).

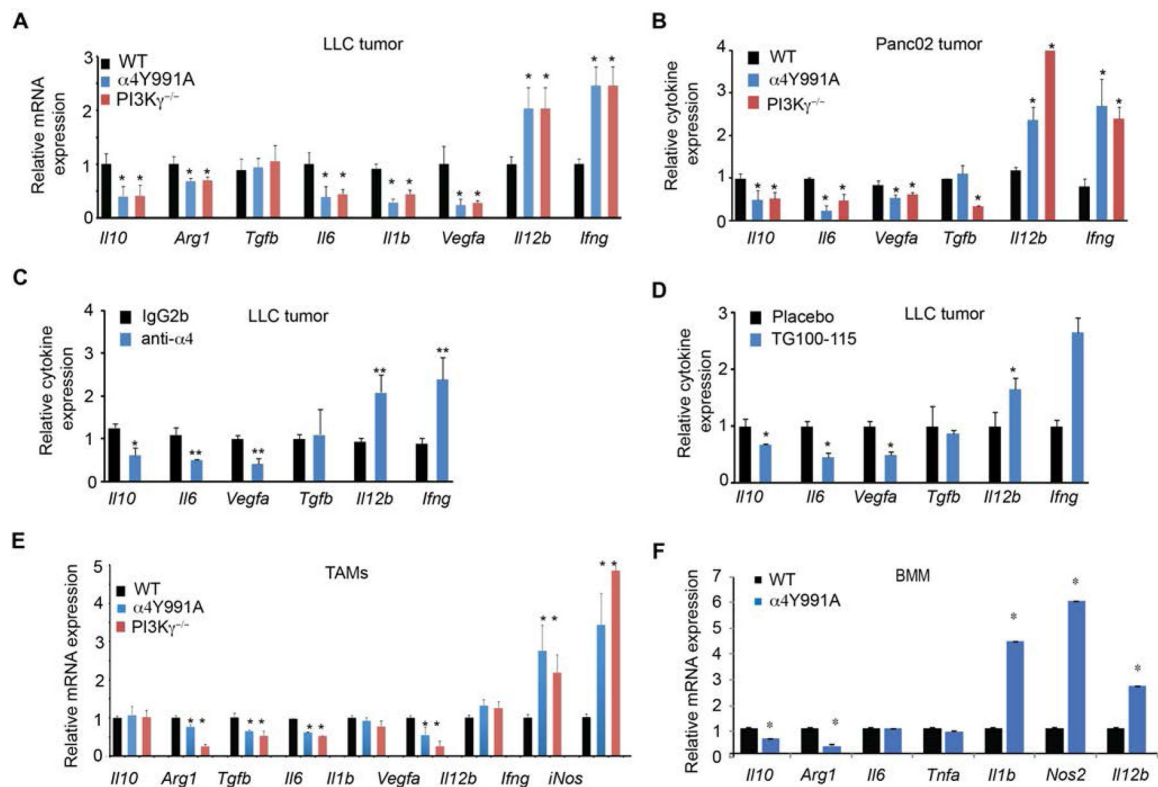


**Figure 3. Blockade of PI3K $\gamma$ -integrin  $\alpha4$  pathway repolarizes tumor associated myeloid cells** (A-B) mRNA expression of immune related cytokines in (A) LLC and (B) Panc02 tumors from WT,  $\alpha4Y991A$ , and  $PI3K\gamma^{-/-}$  mice (n=4) \* $p$ <0.05. (C-D) mRNA expression of immune related cytokines in LLC tumors from mice that were treated with (C) anti- $\alpha4$  versus isotype matched control antibody or (D) PI3K $\gamma$  inhibitor TG100-115 versus control (n=4) \*\* $p$ <0.01. (E) mRNA expression of immune related cytokines in LLC tumor associated myeloid cells from WT,  $\alpha4Y991A$ , and  $PI3K\gamma^{-/-}$  mice (n=4) \*\* $p$ <0.05. (F) mRNA expression of immune related cytokines in in vitro IL-4 stimulated WT and  $\alpha4Y991A$  macrophages (n=4) \* $P$ <0.05. Error bars indicate standard error of the mean (SEM).

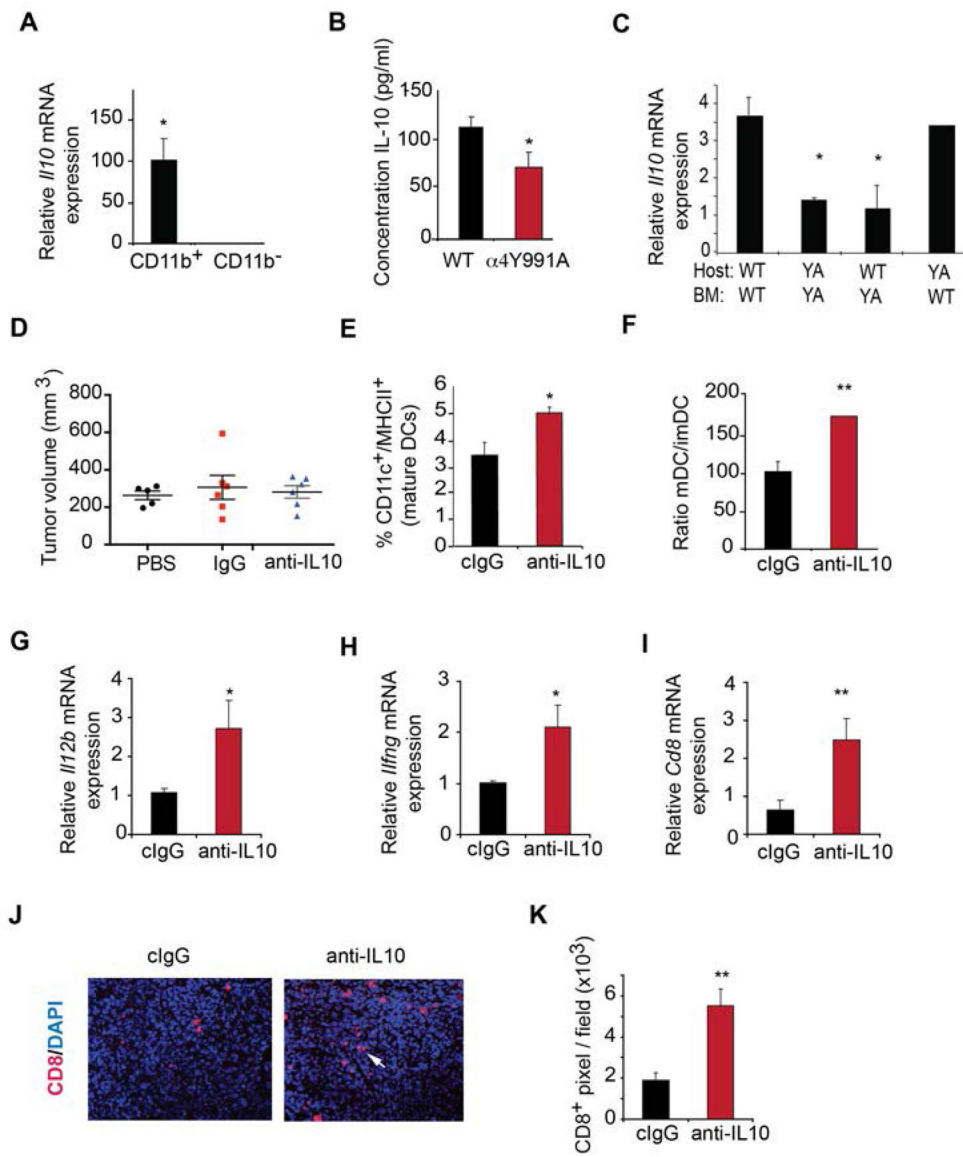


**Figure 4: Integrin  $\alpha 4$  activation controls IL10 expression**

(A) *I10* mRNA levels  $\pm$  SEM in CD11b<sup>-</sup> and CD11b<sup>+</sup> cell populations from LLC tumors (n=3). (B) IL-10 protein concentration (pg/mg total protein)  $\pm$  SEM in LLC tumors from WT and  $\alpha 4$ Y991A animals (n=3) \**p*<0.05. (C) *I10* mRNA levels  $\pm$  SEM in tumors from WT and  $\alpha 4$ Y991A bone marrow transplanted animals (n=3) \**p*<0.05. (D) Mean LLC tumor volumes  $\pm$  SEM from mice that were treated with two doses of anti-IL10 blocking antibody or clgG (n=6) \**p*<0.05. (E) Percent CD11c<sup>+</sup>/MHCII<sup>+</sup> DCs in tumors from D (n=6) \**p*<0.05. (F) Quantification of the ratio of mature DC (CD11c<sup>+</sup>/MHCII<sup>+</sup>) and immature DC (CD11c<sup>+</sup>/MHCII<sup>-</sup>) in mice from D (n=6) \*\**p*<0.01. (G) *I12b*, (H) *Ifng* and (I) *Cd8a* mRNA expression in tumors from D (n=3) \**p*<0.05 \*\**p*<0.01. (J) Representative images of CD8<sup>+</sup> T cells in LLC tumors from D. Scale bar: 100 $\mu$ m. (K) Mean CD8<sup>+</sup> T cells in tumors  $\pm$  SEM (pixels/field) (n=3) \*\**P*<0.01. Error bars indicate standard error of the mean (SEM).

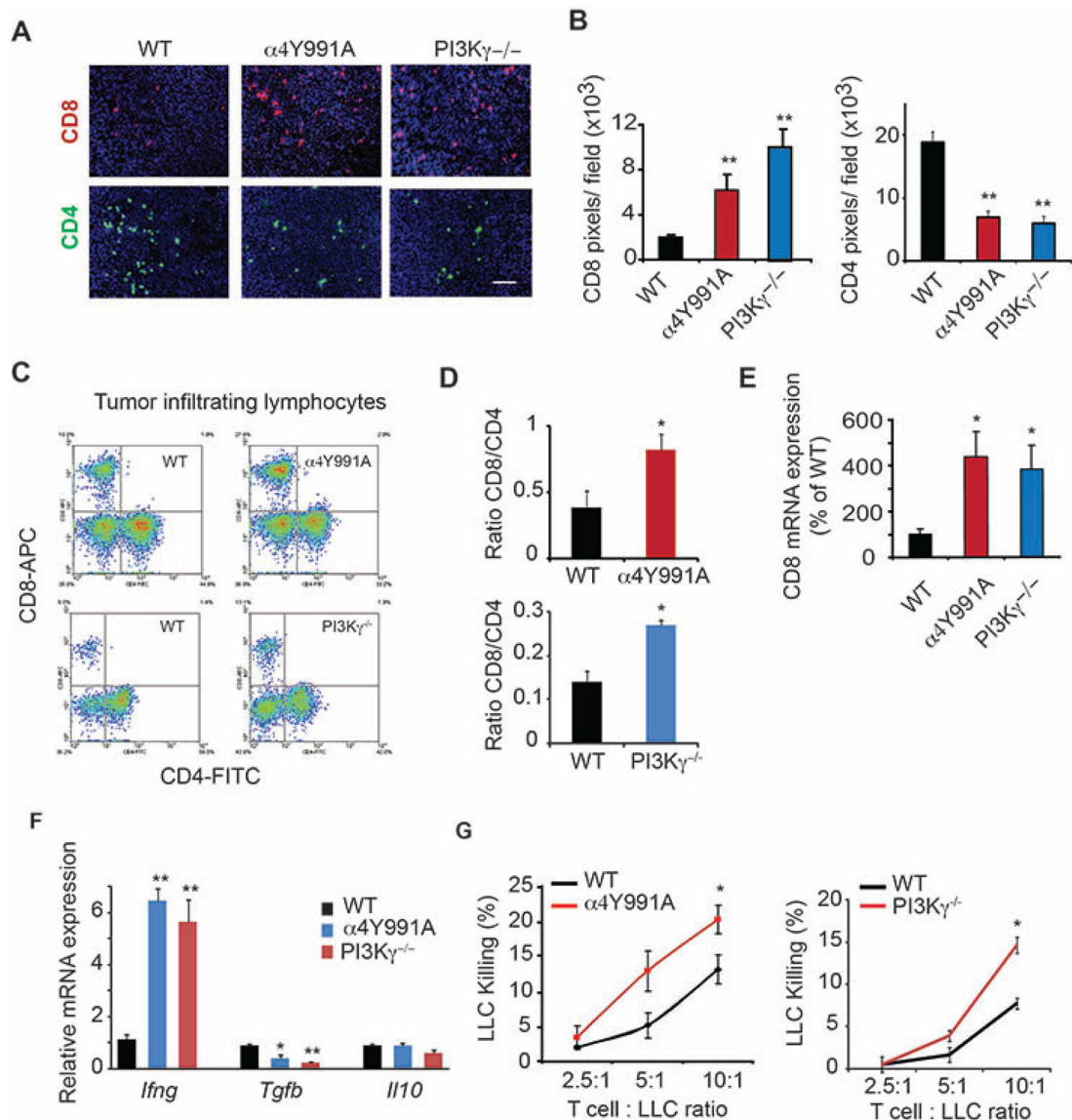


**Figure 5. Blockade of PI3K $\gamma$ -integrin  $\alpha$ 4 pathway promotes CD8<sup>+</sup> T cell infiltration and T cell cytotoxicity**

(A) Representative images of CD4<sup>+</sup> and CD8<sup>+</sup> T cells infiltration in LLC tumors in cryosections from WT,  $\alpha$ 4Y991A and PI3K $\gamma$ <sup>-/-</sup>. Scale bar: 100 $\mu$ m. (B) Quantitative analysis CD4<sup>+</sup> and CD8<sup>+</sup> positive T cells in tumors from WT,  $\alpha$ 4Y991A and PI3K $\gamma$ <sup>-/-</sup> mice (n=5), \*\**P*<0.01 vs WT. (C) Flow cytometry analysis of CD4<sup>+</sup> and CD8<sup>+</sup> tumor-infiltrating lymphocytes from LLC tumor-bearing mice from WT,  $\alpha$ 4Y991A and PI3K $\gamma$ <sup>-/-</sup> animals). (D) The ratio of CD8<sup>+</sup> to CD4<sup>+</sup> T cells in tumors from WT,  $\alpha$ 4Y991A and PI3K $\gamma$ <sup>-/-</sup> animals (n=3), \**P*<0.05 vs WT. (E) Relative expression of *Cd8a* mRNA in TILs from LLC tumors from WT,  $\alpha$ 4Y991A and PI3K $\gamma$ <sup>-/-</sup> animals (n=4), \**P*<0.05. (F) mRNA expression of *Ifng*, *Il10* and *Tgfb* mRNA in TILs from LLC tumors from WT,  $\alpha$ 4Y991A and PI3K $\gamma$ <sup>-/-</sup> animals (n=4). (G) Tumor-infiltrating lymphocytes from LLC tumors from WT,  $\alpha$ 4Y991A and PI3K $\gamma$ <sup>-/-</sup> animals were isolated and mixed with LLC tumor cells. T cell

cytotoxic activity against parental LLC tumor cells was assessed in an ex vivo CTL assay (n=6) \* $P < 0.05$  vs WT. Error bars indicate standard error of the mean (SEM).

Author Manuscript

Author Manuscript

Author Manuscript

Author Manuscript



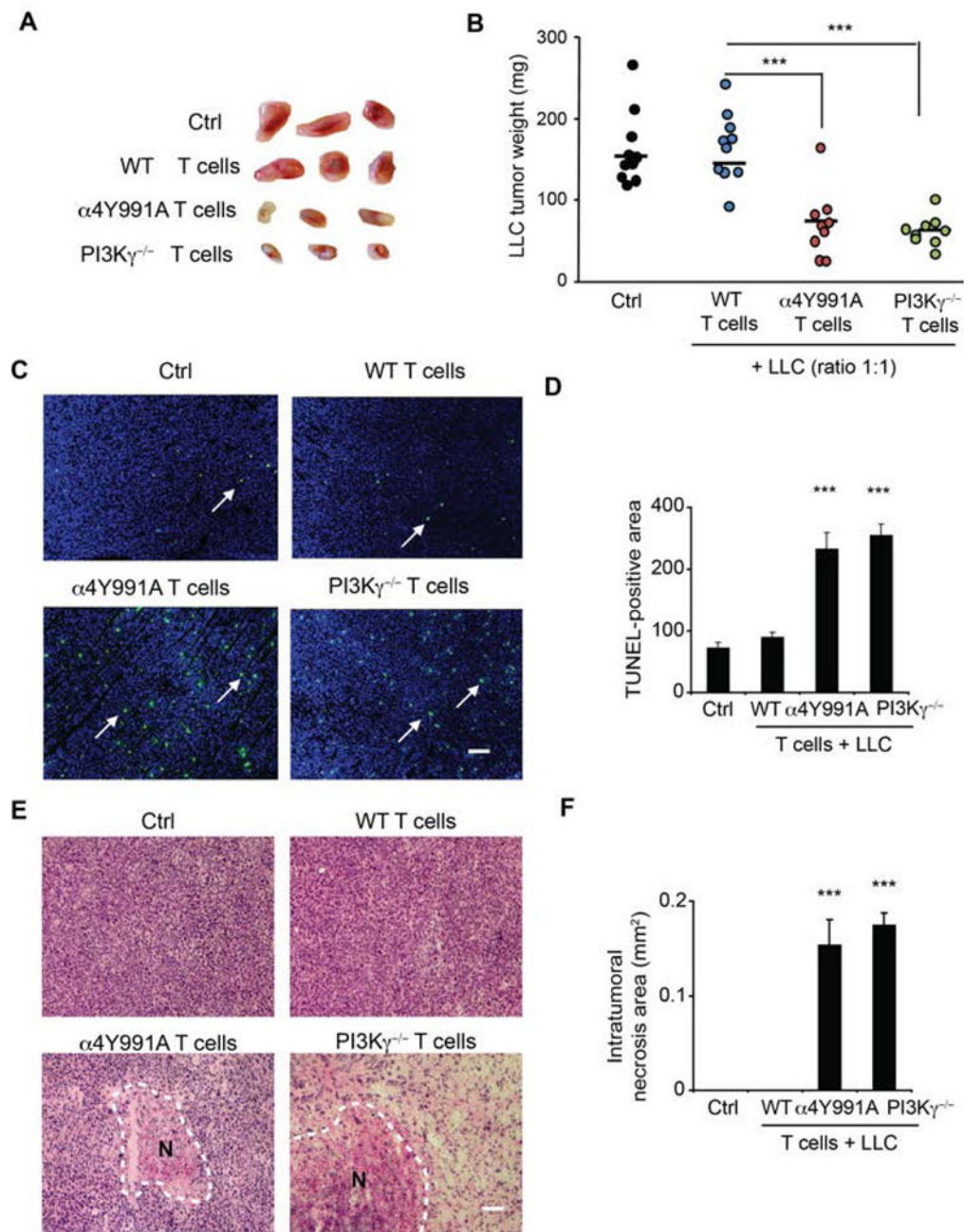


**Figure 6. Blockade of PI3K $\gamma$ -integrin  $\alpha$ 4 pathway stimulates T cell-mediated in vivo tumor cells killing.**

(A) LLC tumor cells were mixed with T cells isolated from LLC tumors grown in WT,  $\alpha$ 4Y991 or PI3K $\gamma^{-/-}$  mice. The mixture was injected in the flank of naïve mice. Representative images of LLC tumors are shown. Scale bar: 1cm. (B) Tumor weights

analyzed after 10 days (n=9–10), \*\*\* $P$ <0.001 vs WT. (C) Representative images of apoptotic cells in LLC tumor by TUNEL immunostaining. (D) Quantification of TUNEL+

cells from C (n=9–10), \*\*\* $P$ <0.001 vs WT. (E) Representative images of necrosis in LLC

tumors from C (n=9–10), \*\*\* $P$ <0.001 vs WT. (F) Quantification of intratumoral necrosis area from E (n=9–10), \*\*\* $P$ <0.001 vs WT.



tumors by H&E staining. **(F)** Quantification of necrotic areas in LLC tumors (n=9–10).  
\*\*\* $P < 0.001$  vs WT. Error bars indicate standard error of the mean (SEM).

Author Manuscript

Author Manuscript

Author Manuscript

Author Manuscript